Critical Insight into Mechanochemical and Thermal Degradation of Imidazolium-based Ionic Liquids with Alkyl and mPEG Side Chains

ARTICLE *in* THE JOURNAL OF PHYSICAL CHEMISTRY C · SEPTEMBER 2014

Impact Factor: 4.77 · DOI: 10.1021/jp504946h

4 AUTHORS, INCLUDING:

Marcello Conte
Anton Paar Tritec SA / EMPA
44 PUBLICATIONS **121** CITATIONS
SEE PROFILE

E. Román
Spanish National Research Council
141 PUBLICATIONS **2,205** CITATIONS
SEE PROFILE

Roman Nevshupa
Spanish National Research Council
60 PUBLICATIONS **302** CITATIONS
SEE PROFILE

THE JOURNAL OF PHYSICAL CHEMISTRY C

Article

pubs.acs.org/JPCC

Critical Insight into Mechanochemical and Thermal Degradation of Imidazolium-Based Ionic Liquids with Alkyl and Monomethoxypoly(ethylene glycol) Side Chains

Maria Mahrova,[†] Marcello Conte,[‡,§] Elisa Roman,[∥] and Roman Nevshupa*[,⊥]

[†]Tribology Unit, IK4-TEKNIKER, C/Iñaki Goenaga 5, 20600 Eibar, Spain

[‡]Anton Paar, Rue de la Gare 4, 2034 Peseux, Switzerland

[§]Laboratory of Materials and Nanostructures, EMPA, Feuerwerkstrasse 39, 3602 Thun, Switzerland

[∥]ICMM-CSIC, C/Sor Juana Inés de la Cruz 3, Madrid 28049, Spain

[⊥]IETCC-CSIC, C/Serrano Galvache 4, Madrid 28033, Spain

Supporting Information

ABSTRACT: Processes of mechanochemical degradation of imidazolium bis((trifluoromethyl)sulfonyl)imide ionic liquids with alkyl and monomethoxypoly(ethylene glycol) (mPEG) side groups were studied using the novel technique of mechanically stimulated gas emission spectroscopy. Mechanical stimulus caused degradation of both the anionic and cationic moieties. For the latter, the degradation was concentrated on the alkyl and ether chains rather than on the imidazole. For the anionic moiety, various degradation steps associated with the emission of CH_xF_y volatile products followed by SO_2 and SO_3 emission were identified. Simulation of frictional heat dissipation revealed that tribochemical reactivity was induced by the mechanical energy supply rather than the temperature increase. Thermal degradation of the same ionic liquids studied using thermogravimetric analysis and Fourier transform infrared spectroscopy was concentrated mainly on the cationic moiety. Thermal stability significantly depended on the side chains. The decomposition of mPEG-functionalized ionic liquids was a two-step process, where the lower temperature step corresponded to mPEG decomposition.

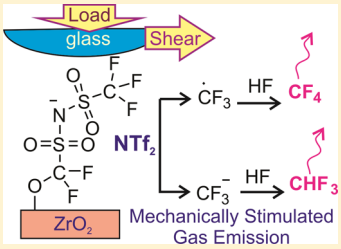

1. INTRODUCTION

Nowadays, ionic liquids (ILs) are used in various advanced industrial applications, e.g., as electrolytes,[1−3] in chemical synthesis and separation processes,[4,5] in catalysis, in nanotechnology, and as engineering fluids.[6] Also, ILs can be used as novel lubricants or lubricant additives,[7−12] especially in extremely clean or harsh environments, e.g., in space, because of their low volatility, low melting point, high thermal stability, high viscosity, and miscibility with organic compounds. A number of studies summarized in comprehensive reviews[13−15] have highlighted different chemical reactivities of the cation and anion moieties under mechanical stimulus. While the anion moiety is usually responsible for reactivity of the ILs with a substrate and formation of protective tribofilms under higher normal loads,[13,16] adsorption of the cation moiety onto the contact surfaces contributes to friction and wear reduction under low and moderate normal loads, conceivably due to formation of a dense surface layer with high viscosity.[13] This hypothesis is supported by the fact that the increase of the chain length of alkyl side groups attached to imidazolium leads to enhancement of the lubricating properties of neat ILs on steel and aluminum.[13,14] Using a vacuum tribometer coupled with a mass spectrometer, Lu et al.[17] showed that the cationic moiety with a longer alkyl chain was more chemically stable on the nascent steel surface. Conversely, on titanium, the lubricating capacities of ILs decreased with increasing length of the alkyl chains, which was related to mechanochemical degradation.[7,18]

Further enhancement of the tribological properties of the ILs can be achieved through functionalization of the cation with poly(ethylene glycol) (PEG), which itself is known to be a good lubricant.[19] However, Gathergood et al.[20,21] have demonstrated that the incorporation of certain functional groups (ethers and, especially, esters) might increase the rate of breakdown of an IL in the environment. Though being a factor of considerable practical importance for environmental sustainability of IL-based lubricants, insufficient chemical stability under heating and mechanical stimulus might be a serious disadvantage, especially for vacuum and space applications, where degradation of a lubricant may cause costly mechanical failure and vacuum environment contamination by volatile products.[22]

Despite the critical importance of the mechanochemical stability of ILs for the performance of advance lubricants, there is still much controversy over the mechanochemical degradation reactions. In part, this can be attributed to the significant

Received: May 20, 2014
Revised: August 7, 2014
Published: September 1, 2014

limitations of the conventional experimental techniques, most of them based on a postmortem approach, for the characterization of nonequilibrium chemical processes occurring in a confined geometry of a sliding interface. Recently, development of mechanically stimulated gas emission (MSGE) spectroscopy has offered a novel tool for in situ and real time characterization of mechano- and tribochemical reactions.[23−29] In this study this technique has been used to investigate the nonoxidative degradation of alkyl- and mPEG-functionalized ILs. For this purpose, commercially available 1-butyl-3-methylimidazolium bis((trifluoromethyl)sulfonyl)imide (IL1) and synthesized α-methoxy-ω-(butylimidazolium)poly(ethylene glycol) bis((trifluoromethyl)sulfonyl)imide (IL2) were used. Study of the thermal degradation of the ILs in the temperature range from 473 to 723 K allowed comparison of the possible chemical reactions relevant to both mechanochemical and thermal degradation of the ILs.

2. EXPERIMENTAL SECTION

2.1. Materials. Monomethoxypoly(ethylene glycol) (mPEG; M_{theory} = 500 g/mol), 1-butylimidazole, and bis(trifluoromethane)sulfonimide lithium salt were purchased from Fluka, Aldrich, and Acros Organics, correspondingly. Pyridine, sodium sulfate, thionyl chloride, 1,4-dioxane (≥99.8%), dichloromethane (≥99.8%), chloroform (≥99.8%), diethyl ether (≥99.8%), and methanol (≥99.8%) were obtained from Sigma-Aldrich. 1-Butyl-3-methylimidazolium bis((trifluoromethyl)sulfonyl)imide, hereinafter referred to as IL1, was synthesized by IoLiTec and used as received. The molecular structures and codifications of the ILs studied in this work are shown in Chart 1.

Chart 1. Structures of the Cations of the Studied Ionic Liquids

IL1 IL2

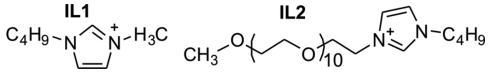

^{1}H, ^{13}C, and ^{19}F NMR spectra of the synthesized products were measured at room temperature at frequencies of 400, 100.6, and 376.5 MHz, correspondingly. For the ^{1}H and ^{13}C NMR analysis, the chemicals were dissolved in $CDCl_3$ (99.8 atom % D) purchased from Armar AG, whereas for ^{19}F NMR, $(CD_3)_2CO$ was used as the solvent. FTIR spectra were recorded using a spectrometer with a Gladi ATR diamond anvil cell.

2.2. Synthesis of α-Methoxy-ω-(butylimidazolium)-poly(ethylene glycol) Bis((trifluoromethyl)sulfonyl)-imide. Synthesis of α-methoxy-ω-(butylimidazolium)poly-(ethylene glycol) bis((trifluoromethyl)sulfonyl)imide, referred to as IL2, was done in three steps following the previously described procedure.[30,31]

2.2.1. Synthesis of α-Methoxy-ω-chloropoly(ethylene glycol). To a solution of methoxypoly(ethylene glycol) (M_{theory} = 500 g/mol) (5.0 g, 9.4 mmol) and pyridine (1.4 g, 18.8 mmol) in 30 mL of 1,4-dioxane was added thionyl chloride (2.24 g, 18.8 mmol) in small portions, maintaining the reaction temperature between 0 and 5 °C. The reaction mixture was stirred at 70 °C for 2 h, then 1,4-dioxane was removed by evaporation, and the obtained crude product was dissolved in dichloromethane and water-washed three times. The collected organic phase was dried with anhydrous Na_2SO_4 and filtrated, and the solvent was evaporated. The yield of the reaction was 4.36 g (94%) of slightly yellow liquid (M_n = 491.01 g/mol). The conformation of the reaction product was probed using NMR: ^{1}H (δ, ppm) 3.71 (t, J = 5.8, 2H), 3.61 (m, 36H), 3.50 (m, 2H), 3.33 (s, 3H); ^{13}C (δ, ppm) 71.9, 71.3, 70.6, 70.5, 70.5, 59.0, 42.7.

2.2.2. Synthesis of α-Methoxy-ω-(butylimidazolium)poly-(ethylene glycol) Chloride. 1-Butylimidazole (1.59 g, 12.82 mmol) was added in small portions to the solution of the previously prepared α-methoxy-ω-chloropoly(ethylene glycol) (3.52 g, 7.16 mmol) in 35 mL of toluene. The reaction mixture was heated under reflux at 110 °C for 90 h. After the reaction mixture was cooled to room temperature, the solvent was evaporated, and the obtained crude product was washed with diethyl ether. Finally, the yellow product was dried in high vacuum, yielding 1.5 g (34%) of a yellow viscous oil (M_n = 615.20 g/mol): ^{1}H NMR (δ, ppm) 10.17 (s, 1H), 7.65 (t, J = 1.8 Hz, 1H), 7.42 (s, 1H), 4.49 (t, J = 4.3 Hz, 2H), 4.17 (t, J = 7.4 Hz, 2H), 3.75 (m, 2H), 3.49 (m, 40H), 3.40 (m, 2H), 3.23 (s, 3H), 1.76 (m, 2H), 1.24 (qd, J = 7.4 Hz, J = 14.8 Hz, 2H), 0.82 (t, J = 7.4 Hz, 3H); ^{13}C (δ, ppm) 137.2, 123.5, 121.6, 71.8; 70.4−70.1, 69.0, 58.9, 49.5, 32.0, 19.4, 13.4.

2.2.3. α-Methoxy-ω-(butylimidazolium)poly(ethylene glycol) Bis((trifluoromethyl)sulfonyl)imide. The previously prepared α-methoxy-ω-(butylimidazolium)poly(ethylene glycol) chloride (0.49 g, 0.72 mmol) was dissolved in a mixture of 6 mL of methanol with 2 mL of water. Bis(trifluoromethane)-sulfonimide lithium salt (0.41 g, 1.44 mmol) was added in one portion. The reaction mixture was continuously stirred at room temperature for 96 h. After removal of the solvent, the obtained yellow product was dissolved in 15 mL of dichloromethane and washed with water several times. The combined organic phase was dried with anhydrous Na_2SO_4 and filtrated. After solvent evaporation, the yield of the synthesis was 0.59 g (92%) of a yellow viscous oil (M_n = 887.89 g/mol): ^{1}H NMR (δ, ppm) 8.91 (t, J = 1.6 Hz, 1H), 7.60 (t, J = 1.8 Hz, 1H), 7.36 (t, J = 1.8 Hz, 1H), 4.40 (t, J = 4.3 Hz, 2H), 4.20 (t, J = 7.5 Hz, 2 H), 3.85 (t, J = 4.6 Hz, 2H), 3.66−3.60 (m, 40H), 3.55 (t, J = 5.2 Hz, 2H), 3.38−3.37 (m, 3 H), 1.90−1.82 (m, 2H), 1.38 (qd, J = 7.4 Hz, J = 14.8 Hz, 2H), 0.98 (t, J = 7.4 Hz, 3 H); ^{13}C NMR (δ, ppm) 136.0, 123.5, 121.9, 119.7 (q, J_{C-F} = 321.4 Hz), 71.8, 70.4−70.2, 68.6, 58.9, 49.7, 31.9, 19.3, 13.3; ^{19}F NMR (δ, ppm; $(CD_3)_2CO$) −79.94 ($N(SO_2CF_3)_2$).

The characteristic quartet at 119.7 ppm (q, J_{C-F} = 321.4 Hz, CF_3) observed in the ^{13}C NMR spectrum corresponds to the CF_3 groups of the anion moiety. The ^{19}F NMR spectrum showed a signal at −79.94 ppm that indicates the presence of the required bis((trifluoromethyl)sulfonyl)imide anion (NTf_2).

FTIR analysis of IL2: ν_{max}(diamond anvil cell)/cm^{-1} (T, %) 3147.30 (95.31) (N^+), 2873.47 (76.29) (CH_3−O, ν(C−H alkane), O−CH_2−O, CH_2−N), 1565.46 (89.99) (ν(C═N)), 1454.06 (86.1) (δ_s(CH)), 1349.63 (45.51) (ν(R−SO_2−N)), 1333.05 (60.25), 1226.81 (71.71) (ν(C−N)), 1183.09 (27.57) (ν(C−F)), 1132.63 (33.61) (ν(S═O)), 1094.85 (29.78) (CH_2−O−CH_2), 1054.26 (23.06) (ν(C−F)), 947.75 (67.95) (ν(C−O)), 847.59 (73.49) (ρ(CH_2),[32] γ(C4−H)[33]), 787.36 (76.14) (CF_3), 760.83 (80.87), 739.23 (73.35) (γ(C−H imidazole)), 652.81 (73.15) (ν(C−S)), 614.77 (42.64) (C−H imidazole), 599.63 (47.69) (C−H imidazole), 569.40 (41.41) (C−H imidazole), 510.34 (48.12) (ω(CF_2)).

2.3. Characterization Techniques for Thermal Degradation. Differential scanning calorimetry (DSC) was carried out under nitrogen gas flow at a rate of about 50 mL min^{-1}

dx.doi.org/10.1021/jp504946h | J. Phys. Chem. C 2014, 118, 22544−22552

using closed aluminum pans with a small hole in the lids. The thermal behaviors were determined through a cycle from 243 to 433 K at a heating rate of 10 K min^{-1}. For thermogravimetric analysis (TGA), the samples of the ILs were heated in open platinum pans from 298 to 873 K with a heating rate of 10 K min^{-1} under a nitrogen flow rate of 50 mL min^{-1}. Before both DSC and TGA, the samples were kept at 393 K for 20 min to eliminate the volatile components of the ILs.

To shed light on the mechanisms of thermal degradation, ATR FTIR spectra were measured for the samples of ILs which had been heated at different temperatures in a nitrogen atmosphere and then cooled to room temperature. For this purpose six samples (15−20 mg) of each IL were placed in open platinum pans and heated from 298 to 473, 523, 573, 623, 673, and 723 K, correspondingly, with a heating rate of 10 K min^{-1} under a nitrogen flow rate of 50 mL min^{-1}.

2.4. MSGE Spectroscopy. The chemical reactivity of ILs under pure mechanical action, i.e., without additional heating, was studied using MSGE spectroscopy and the original experimental system TriDes. This technique is based on the mass spectrometry analysis of the gases and volatiles emitted from the material—IL in this study—under well-controlled reciprocating sliding in ultrahigh vacuum. The description of both this technique and the experimental procedure can be found elsewhere.[22,34−36]

Polished yttria-stabilized zirconia (YSZ) flat sheets were used as substrates for the ILs under study. YSZ and borosilicate glass were selected for the substrate and the pin because of their low reactivity and negligible gas emission under mechanical stimulation as was probed in the preliminary tests by sliding the pin against the bare substrate. The substrates were cleaned consequently in acetone and 2-propanol ultrasonic baths and dried in a nitrogen stream. Since both ILs have high viscosity at room temperature, before deposition on the substrate, the ILs were dissolved in $CHCl_3$. A drop of approximately 1 μL of the solution was placed on the substrate and extended over its surface using a glass bar. To eliminate the solvent, the ILs were degassed before the experiment in a load-lock chamber at a pressure below 10^{-5} mbar. A borosilicate glass sphere, 3 mm in diameter, was used as a pin for performing reciprocating sliding of the IL-covered substrates under the applied normal load of 9.8 N and mean sliding velocity of 2.7 mm s^{-1}.

After introduction of the sample and before the experiments were started, the system was kept for several hours with a quadrupole mass spectrometer (QMS) on to establish the equilibrium base pressure. Then spectra of the residual gases were acquired previous to, in the course of, and after sliding. At least five spectra were acquired previous to rubbing to have a representative data sample for determination of the mean value, $\overline{I}_b(m/z)$, and standard error of the mean, $se_b(m/z)$, for each spectral component with mass-to-charge ratio m/z. DMS (differential mass spectrometry) spectra during sliding and afterward were obtained from the measured mass spectra by subtracting $\overline{I}_b(m/z)$:

$$\Delta I(m/z, t) = I(m/z, t) - \overline{I}_b(m/z) \quad (1)$$

Therefore, a DMS spectrum represents variations of the spectral components in a certain moment of time due to the effect of mechanical action. Furthermore, to discard random variations, the following filtration procedure was applied to the DMS spectra:

$$\Delta I(m/z, t) = \Delta I(m/z, t) \quad \text{if} \quad \Delta I(m/z, t) > 5[\mathrm{SN}(m/z, t)] \quad (2a)$$

$$\Delta I(m/z, t) = 0 \quad \text{if} \quad \Delta I(m/z, t) \le 5[\mathrm{SN}(m/z, t)] \quad (2b)$$

where $\mathrm{SN}(m/z,t) = I(m/z,t)/se_b(m/z)$ is the corresponding signal-to-noise ratio of the m/z-th spectral component at time t.

3. RESULTS AND DISCUSSION

3.1. Thermal Decomposition. The ILs under study were liquid at room temperature. No significant phase transitions were detected in the temperature range from 293 to 523 K as can be inferred from the DSC scans shown in Figure 1. The

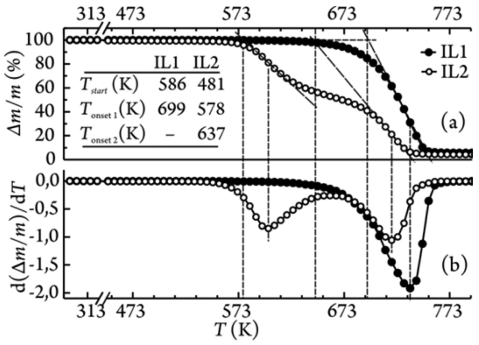

Figure 1. (a) Relative remaining mass ($\Delta m/m$) of the ILs as a function of temperature. (b) Derivative of the relative mass loss with temperature. The intersections of the tangent dashed lines with the horizontal one determine the onset temperatures.

start temperature of decomposition, T_{start}, and the onset temperature, T_{onset}, were determined from the DSC graphs and are listed in the inset in Figure 1a. The oligomer-linked IL2 is stable up to 481 K, while IL1 with alkyl groups is stable up to 586 K. The determined onset temperature for IL1 is consistent with those of previous studies.[37,38] The decomposition of IL2 was a two-step process, while for IL1 there was only one step.

Graphs in Figure 2 show the portions of the FTIR spectra in the ranges between 450 and 1900 cm^{-1} and between 2500 and 3800 cm^{-1} for the ILs heated at various temperatures. The most significant spectral features have been assigned on the basis of the available published data.[33,39−43] (For details see Figure S1 in the Supporting Information.) The FTIR spectra of the anionic moiety of IL1 were almost unchanged in the entire range of the heating temperatures (Figure 2 a). For the cationic moiety of IL1 (Figure 2 b), some variations were found right after heating at 723 K. At this temperature the intensity of the bands in the range between 3160 and 3200 cm^{-1}, which are associated with alkyls, slightly decreased, while two new broad bands centered at 3260 and 3558 cm^{-1} appeared. These results differ from those of the previous work of Kroon et al.,[37] who studied thermal degradation of IL1 using quantum chemical simulation. They found that ILs that contain non-nucleophilic anions, such as NTf_2, cannot decompose via dealkylation and the cation stays intact.

For IL2, significant variations in FTIR spectra occurred for both the cation and anion moieties (Figure 2 c,d). At temperatures higher than 623 K, i.e., after the first thermal degradation step (Figure 1b), the initially strong bands at 949 cm^{-1} (ν(C−O)), 1094 cm^{-1} (ν(CH_2−O−CH_2)), and 2874 cm^{-1} (ν(C−H)) completely vanished. Since all the above

dx.doi.org/10.1021/jp504946h | J. Phys. Chem. C 2014, 118, 22544−22552

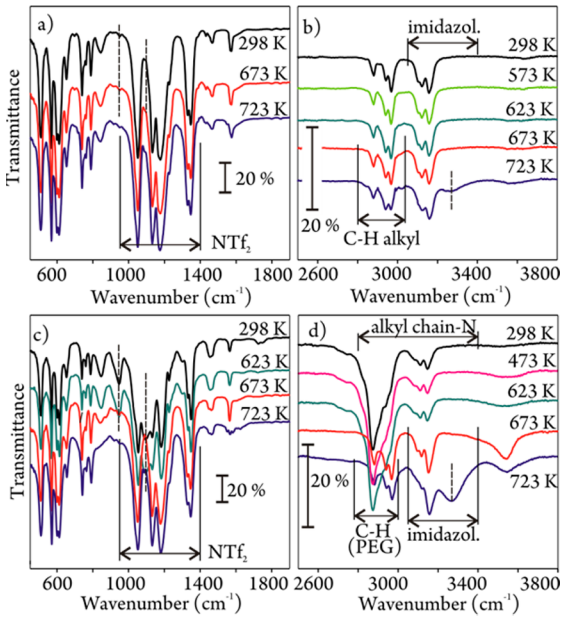

Figure 2. ATR FTIR spectra of IL1 (a, b) and IL2 (c, d) after heating to various temperatures shown on the graphs. Note the different vertical scales on the graphs.

bands are associated with mPEG, this step can be linked to mPEG decomposition. This suggestion is also supported by the fact that the onset temperature of IL2 decomposition coincides with the onset temperature of PEG pyrolysis.[44] Once the bands of mPEG died away at $T > 623$ K, the anion bands of IL2 in the region of 1010−1400 cm^{-1}, i.e., the bands ascribed to C−F, C−N, and S═O stretching vibrations, became very similar to those of IL1. The bands of stretching vibrations of C−H of imidiazole remained unchanged until 623 K and slightly decreased at higher temperatures. This also agrees with previously published results which pointed to the imidazole group as one of the most stable components of the ILs.[13,17,37] At temperatures above 623 K, the bands assigned to C−H vibrations of the groups other than imidazole (alkanes, glycol, etc.) decreased, although the extent of the decrease differed for various vibration modes: it was minor for stretching (2879 and 2940 cm^{-1}), moderate for in-plane symmetrical bending (1463 cm^{-1}), and significant for rocking and out-of-plane (847 cm^{-1}) modes.[32,33,45,46] The last band deserves special attention because of the fundamental difference between the two ILs concerning the behavior of this band with temperature. While for IL1 the band was invariant in the studied temperature range, for IL2 (Figure 2c), it decreased with increasing temperature and completely vanished at 723 K. Bearing in mind that IL1 has no CO bonds, it is possible to ascribe the band at 847 cm^{-1} to out-of-plane deformation of CH in C4 and C5 alkyls[33] and rocking of CH_2 in butyl.[47] For IL2, this band can be a superposition of the same vibration modes of CH_2 of both butyl and mPEG (gauche form) and CO stretching motion in mPEG.[32,45,46] Dying away of the band at 847 cm^{-1} at temperatures higher than the decomposition of mPEG suggests a decrease of the chain length of alkyl groups of IL2 since the band of the stretching motion of CH did not change significantly with temperature. This is a quite unexpected result implying that the poly(ethylene glycol) degradation could trigger degradation of butyl side groups in IL2. Although, with limited data, this finding needs to be interpreted with caution, it could be linked with radical chain reactions such as depolymerization and random backbone chain scission, which are responsible for poly(ethylene glycol) decomposition at temperatures above 573 K.[48] The end radicals formed in these processes may further abstract hydrogen or methyl from butyl, yielding shorter alkyl or alkene chains and various volatile products including monomers, ethyl and methyl alcohol, and noncyclic ethers.[48,49]

A new broad band with the maximum at 3270 cm^{-1} appeared at 723 K for both liquids, being somewhat stronger for IL2 (Figure 2d). Plausible explanations for this band might be that some NH-containing molecules are released as a result of partial imidazole degradation[50] and some alkenes are formed in thermal degradation of alkyl groups. A contribution to this band from the OH of alcohols as the degradation products of poly(ethylene glycol)[48] can also be expected for IL2. In addition, another new broad band centered at 3537 cm^{-1} was

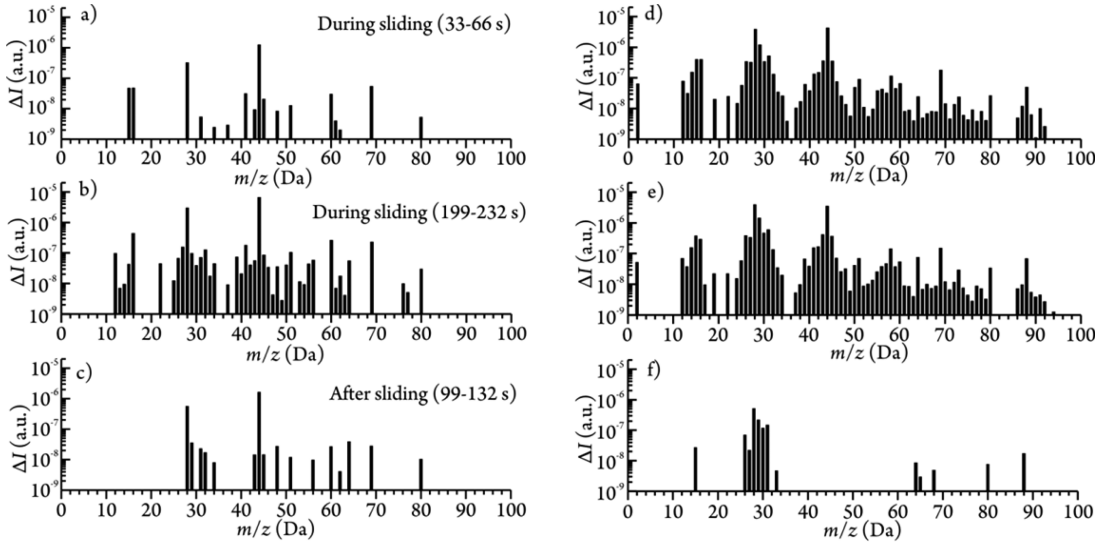

Figure 3. Differential mass spectra of MSGE from IL1 (a−c) and IL2 (d−f) during mechanical stimulation and afterward. Spectra a, b, d, and e were obtained during sliding: (a, d) in the time interval from 33 to 66 s from the beginning of sliding; (b, e) in the time interval from 199 to 232 s from the beginning of sliding. Spectra c and f were obtained during the rest period, in the time interval from 99 to 132 s after the end of sliding.

dx.doi.org/10.1021/jp504946h | J. Phys. Chem. C 2014, 118, 22544−22552

observed at 473 K for IL2. This band reached its maximum at 673 K and slightly decreased at 723 K. For IL1, this band was much weaker. This band could not be confidently identified in this study.

The lower nonoxidative decomposition temperature of IL2 compared to IL1 can be due to the combination of a bulky asymmetric cation, in which the poly(ethylene glycol) chain is linked to the imidazole ring, and a relatively small anion. The ether oxygen atoms can associate with the hydrogen atoms of the imidazole ring and weaken ionic interactions between the imidazolium cation and NTf_2, thus decreasing the lattice potential energy of IL2.[29] There are similarities between the findings of this study and those described by Minami,[13] who reported that higher alkyl groups in imidazolium cause a decline in the thermo-oxidative stability while improving the tribological properties.

While the NTf_2 anion and 1-butyl-3-methylimidazolium were stable up to 586 K and the cation degraded only slightly at temperatures as high as 723 K, incorporation of an mPEG group into the cation drastically reduced the nonoxidative thermal stability of the cation moiety. There is evidence that mPEG thermal degradation could also induce decomposition of butyl side groups.

3.2. In Situ Characterization of the Tribochemical Reaction Using MSGE Spectrometry. Filtered DMS spectra corresponding to different rubbing durations or different time periods elapsed after the rubbing termination for both IL1 and IL2 are shown in Figure 3. Though accurate identification of all molecular and radical volatile components as the products of mechanically induced degradation of the ILs is not an easy task because of superposition of ion fragments of various molecules in the DMS spectra, some of these components can be identified quite confidently. The groups of peaks at m/z 12−16, 26−29, and 38−44 Da in Figure 3a,b can be ascribed to a mixture of C1, C2, and C3 alkanes and alkyl radicals. Strong peaks at m/z 28 and 44 Da and the peak at m/z 22 Da can also have contributions from CO^+, CO_2^+, and CO_2^{2+}, correspondingly. The presence of higher alkenes, probably C5 and/or C6, can be inferred from the peaks at m/z 53−56, 76, 77, and 83 Da. The peak at m/z 76 Da can be assigned to 1-fluorobutane. The peaks at m/z 31, 33, 34, 50, 51, and 69 Da can be identified as CF^+/CH_3O^+, CH_2F^+, CH_3F^+, CF_2^+, CHF_2^+, and CF_3^+, correspondingly. The peaks at m/z 60−63 Da appear to suggest the presence of volatile methanesulfenic acid (CH_3SOH), dimethyl sulfoxide ($(CH_3)_2SO$), and difluoroethene ($C_2H_2F_2$) or their radicals. Also, although less likely, these peaks can be assigned to aromatic groups, the formation of which in alkanes under high shear stress was reported by Cheng et al.[51] The peaks at m/z 32, 48, 64, and 80 Da can be attributed to S^+/CHF^+, SO^+, SO_2^+, and SO_3^+/CH_3SOH^+, respectively.

For IL2 (Figure 3d,e), in addition to the above peaks, which were generally more intensive than for IL1, hydrogen and various products of PEG degradation could be identified. The products of nonoxidative pyrolysis of PEG typically include ethyl and methyl alcohols, various alkenes, noncyclic ethers, formaldehyde, acetic aldehyde, ethylene oxide, CO, CO_2, etc.,[48] all of which have peaks in the range between 12 and 75 Da. The peaks with $m/z > 75$ Da may correspond to various fragments containing three and more ethylene oxide monomers. Noticeable hydrogen desorption occurred during friction, as follows from the peak at 2 Da. In contrast to the earlier findings of Lu et al.,[17] H_2 emission has not been found for alkyl-functionalized imidazolium. Interestingly, the peaks at m/z 17 and 18 Da, corresponding to water, were observed to steeply decrease at the beginning of rubbing. The initial decrease became less pronounced while rubbing continued and vanished after approximately 100 s. For IL1, no variation in these peaks could be found.

When sliding finished, the peaks decreased, although with different rates (Figure 3c,f). Some of the peaks remained for more than 100 s after the end of sliding. Similar behavior can also be seen at the beginning of sliding, when the intensity of various peaks increased with different rates. Taken together, these findings suggest different processes and reactions behind the emission of various degradation products. To better understand these processes, the signals of the DMS spectra were plotted vs time. Figure 4 shows some of the most representative behavior patterns (BPs) of the components of the DMS spectra.

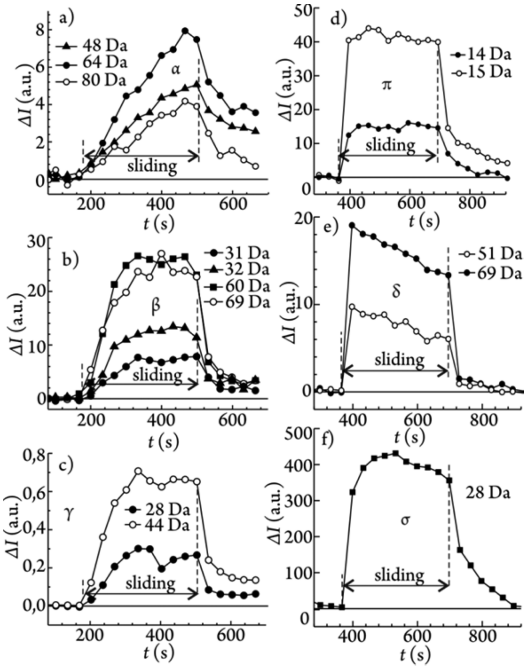

Figure 4. Most representative time behavior patterns of various components of DMS spectra: (a−c) IL1; (d−f) IL2. (a) Pattern α. The ion fragments with m/z 48, 64, and 80 Da can be ascribed to SO^+, SO_2^+, and SO_3^+, correspondingly. (b) Pattern β. The ion fragments with m/z 31, 32, and 69 Da can be ascribed to CF^+, CHF^+, and CF_3^+, correspondingly. (c) Pattern γ. The ion fragments with m/z 28 and 44 Da can be ascribed to $CO^+/C_2H_4^+$ and $CO_2^+/C_3H_8^+$, correspondingly. (d) Behavior pattern of alkanes and/or alkyl radicals emitted due to sliding. The ion fragments with m/z 14 and 15 Da can be ascribed to CH_2^+ and CH_3^+, correspondingly. (e) Pattern δ. The ion fragments with m/z 51 and 69 Da can be ascribed to CHF_2^+ and CF_3^+, correspondingly. (f) Pattern σ. The ion fragments with m/z 28 Da can be ascribed to $CO^+/C_2H_4^+$.

For the spectral components with m/z 48, 64, and 80 Da for both ILs and m/z 88 for IL2, the increase during sliding was gradual so that a steady state was not reached in more than 300 s. The decrease after the end of sliding was also gradual: in 100 s the signals were still far from zero. This gradual behavior has been denoted as pattern α. For all other spectral components of IL1, a steady regime was reached after 60−120 s of rubbing. During the steady regime some oscillations around the mean or a certain drift of the mean could be observed for various

dx.doi.org/10.1021/jp504946h | J. Phys. Chem. C 2014, 118, 22544−22552

Table 1. Correspondence of Ion Fragments to Various Behavior Patterns

BP	IL1	IL2
α	48, 64, 80	48, 64, 80, 88
β	12−16, 22, 25−27, 29−34, 37, 39, 40−43, 45, 46, 49−51, 53−57, 60−63, 66, 69, 72, 76, 83	13, 25, 26, 29−33, 37, 40, 42, 53, 54, 57, 58, 65−67, 68, 70, 73−75, 86
γ	28, 44	
π		14, 15, 19, 22, 24, 27, 34, 39, 41, 47, 52, 55, 63, 72, 87, 89, 91, 92, 94
δ		2, 16, 44, 50, 51, 59−62, 69
σ		12, 28, 43, 45, 46, 56
ν		17, 18

components. After the end of sliding the signals decreased and in 60−120 s reached new much lower steady values, which, however, were not zero. The signals continued to decrease quite slowly, returning to the initial value after tens of minutes. This behavior pattern has been denoted β. It should be mentioned that for the components with m/z 28 and 44 Da the remaining steady-state intensity after the end of sliding was especially high, up to 21% of the steady value during sliding. Therefore, this behavior pattern was singled out from group β and denoted γ. The transient processes at the beginning of sliding and after its end were much slower than the pressure transients due to the pumping process.

For IL2, five behavior patterns have been identified: α and β, already described, and three new patterns, π, δ, and σ. With the exception of the initial very steep increase at the beginning of sliding, pattern π is similar to pattern β. Pattern δ is characterized by a steep increase at the initial moment of rubbing followed by an almost linear decrease during rubbing and a steep decrease after the end of rubbing. The signals returned to the initial values in less than 100 s. Finally, some spectral components have complex behavior which seems to be a combination of two or several basic patterns—pattern σ. Table 1 classifies by the defined behavior patterns all spectral components of the DMS spectra for both ILs.

These findings provide strong evidence for degradation under tribological activation of both the cationic and anionic moieties of the ILs. In the case of the cationic moiety, the degradation is concentrated on the alkyl and ether chains rather than on the imidazole. These conclusions are consistent with those reported by Lu et al.[17] for decomposition under steel/steel friction in vacuum of two 1-alkyl-3-methylimidazolium bis((trifluoromethyl)sulfonyl)imide ILs.

3.3. Discussion. Among the factors, which are traditionally considered by many authors as the most relevant for the mechanochemical degradation of the ILs,[7,52−54] the following two can be definitely ruled out: catalytic effect of nascent metal surfaces and frictional heating. The former has been discarded because both the pin and the substrate were bulk oxides. As for the latter one, the model[52] of heat dissipation at a unlubricated sliding contact predicts the maximum temperature increase after one cycle of only 3.84 K. (See the data used for modeling and the results in Table S1 in the Supporting Information.) Considering heat sink through the massive metal sample holder and heat diffusion through the IL, the maximum total surface temperature after various hundreds of friction cycles at the end of the experiment can hardly exceed 313 K, which is much below the start temperature for the IL's thermal decomposition.

On the other hand, mechanical stimulation on the contact zone can supply highly concentrated mechanical energy to the IL, allowing bond dissociation and formation of ions and radicals.[53,54] These fragments can either desorb—and, thus, be directly registered by a QMS—or further chemically react with the components of the IL and/or the substrate surface, producing different volatile species.

With limited experimental data, definitive conclusions on the mechanochemical reactions lying behind the degradation of such a complex system as confined ILs under shear stress could not be reached in this study. However, a hint for deciphering these reactions has been obtained by adopting a reasonable assumption on the coherent behavior of the mass spectral species originating from the same emitted volatile components. The dissimilar behavior for the two groups of ions, (i) S^+, SO^+, SO_2^+, and SO_3^+ and (ii) CF^+, CHF^+, CF_2^+, and CF_3^+, has suggested that, although these ions come from the same anionic moiety, they correspond to different volatile decomposition products. Thus, mechanically induced degradation of NTf_2 is, conceivably, a multistep reaction rather than one-step detachment of a volatile triflyl group through the cleavage of the S−N bond. This degradation reaction should be different from that proposed by Kroon et al.,[37] who reported that the anion breakdown has to occur via SO_2 release, since CF_x emission anticipates the emission of SO_2 for IL1.

Since frictional heating seems to be irrelevant in our case, mechanical stress could be the main activation factor. This suggestion is supported by a number of studies demonstrating that NTf_2 can be easily immobilized on a hydroxylated oxide surface (Scheme 1),[55−57] e.g., normal YSZ with a natural surface hydroxyl layer, whereas the alkylated imidazolium cation is considered mobile. Shear stress, τ, applied to the anchored anion can reduce the thermal energy required for the bond breaking and increase the rate of the mechanochemical reaction, Q:[58]

$$Q \propto \exp\left(-\frac{\varepsilon - \nu\tau}{kT}\right) \quad (3)$$

Scheme 1. Possible Reaction of NTf_2 with the Substrate and First Decomposition Step under Mechanical Stimulus

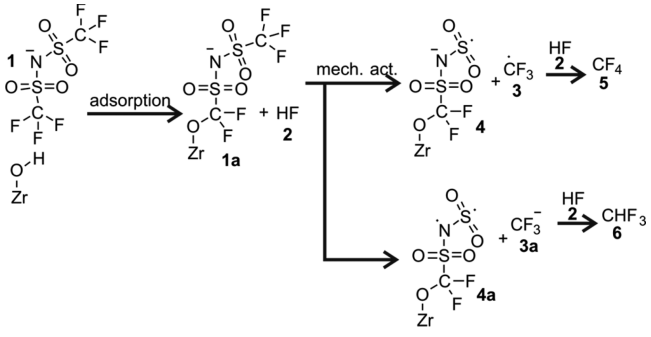

dx.doi.org/10.1021/jp504946h | J. Phys. Chem. C 2014, 118, 22544−22552

where ε is the binding energy, k is Boltzmann's constant, T is the temperature, and ν is the material constant. The decomposition of anchored NTf_2 can start from the detachment of the CF_3 group (Scheme 1) in a radical (**3**) or an ion (**3a**) form at the free end of NTf_2 since the C−S bond is the weakest in the triflyl group.[59,60] CF_3 can further react with HF (**2**), yielding CF_4 (**5**) or CHF_3 (**6**). Both CF_4 and CHF_3 have characteristic mass spectrometry peaks at 19, 31, 32, 50, 51, and 69 Da observed in this study.

The presence of SO_3 in the emitted gases may indicate that the remaining fragment (**4** or **4a**) further reacts with the substrate. Slow emission kinetics of SO_2 and SO_3 also support the hypothesis of surface reactions with desorption being the rate-limiting step.

Despite the fact that the anionic moiety was the same for both ILs, the degradation of the anionic moiety was slightly different for the two liquids. This can be inferred from different emission behaviors of various fluorinated ions with m/z 19, 50, 51, and 69 Da: β for IL1 and $\pi + \delta$ for IL2. The 30% decrease in the emission rate (pattern δ) cannot be explained by depletion of NTf_2 in IL2 during the experiment since the quantity of the emitted molecules (several tens of nanomoles) was below 1% of the total amount of IL2 on the substrate surface. Likely, the decrease in the emission rate can be associated with competitive adsorption on the substrate of the NTf_2 and the products of mPEG decomposition.

As for the cationic moiety, mechanical stress can also cause the detachment of alkyl groups even though the cation is considered mobile. This is because the relaxation time of ILs with imidazolium cations is slow,[61] so that the nanoscale heterogeneities can persist over many nanoseconds. The relaxation time can be even higher if the cations of imidazolium-based ILs bond with each other in the presence of nucleophilic anions, such as F^-.[37] Therefore, the cation can be significantly strained under external normal load combined with shear deformation.

The results of this study suggest that various surface reactions can be crucial for the lubricating properties and low-temperature mechanochemical stability of ILs. These reactions may include (i) water adsorption on hydrophilic ether groups of IL2 under mechanical agitation, (ii) possible competitive adsorption on the substrate of NTf_2 and mPEG decomposition products, and (iii) emission of CO_x. Though emission of CO_x as one of the degradation products of mPEG is quite expectable for IL2, generation of these gases under mechanical activation of IL1 suggests oxidation of the alkyl groups on the substrate surface.

Future research should therefore concentrate on the investigation of the possible surface chemical reactions of the ILs and their components with oxides under shear stress.

CONCLUSIONS

TGA has shown that for the reference IL the NTf_2 anion and 1-butyl-3-methylimidazolium were stable up to 586 K while the cation degraded only slightly at 723 K. Incorporation of an mPEG group into the cation drastically reduced its non-oxidative thermal stability: the start temperature decreased to 481 K. The decomposition of the mPEG-functionalized IL was a two-step process, where the low-temperature step corresponded to mPEG decomposition. There is evidence that the chain radical reaction of PEG thermal decomposition could also induce butyl group decomposition.

MSGE spectrometry showed that both the cationic and anionic moieties of the ILs degrade under tribological activation. In the case of the cationic moiety, the decomposition is concentrated on the alkyl and ether chains rather than on the imidazole. Decomposition of the anionic moiety was associated with the release of CF_x, CH_xF_y, and SO_x volatile products. In contrast to the assumed thermal decomposition mechanisms, emission of CF_x and CH_xF_y anticipated the SO_x emission. This can be explained by possible reaction of the anion fragment with the substrate, where SO_x desorption is the rate-determining step. From the different emission behaviors of CF_x, CH_xF_y, and SO_x, it was concluded that the anion decomposition has to be a multistep reaction rather than one-step detachment of the volatile triflyl group through the cleavage of the S−N bond. The presence of volatile methanesulfenic acid (CH_3SOH), dimethyl sulfoxide ($(CH_3)_2SO$), and difluoroethene ($C_2H_2F_2$) may indicate possible reactions between the degradation products of both moieties.

On the basis of modeling of frictional heat dissipation, it was concluded that the temperature increase at contact has to be insignificant to produce thermal decomposition. The observed decomposition of the ILs must be associated with the supply of highly concentrated mechanical energy to the IL, allowing bond dissociation and formation of ions and radicals.

ASSOCIATED CONTENT

Supporting Information

Additional ATR FTIR spectra of the ILs at room temperature with the most features identified and initial data and calculation results of the flash temperature in sliding contact. This material is available free of charge via the Internet at http://pubs.acs.org.

AUTHOR INFORMATION

Corresponding Author

*E-mail: r.nevshupa@csic.es.

Notes

The authors declare no competing financial interest.

ACKNOWLEDGMENTS

We acknowledge the funding provided by the Basque Government and the Ministry of Economy and Competitiveness of Spain under Projects RYC-2009-04125, BIA2011-25653, and IPT-2012-1167-120000 with the participation of the European Regional Development Fund (FEDER). We are grateful to Dr. A. Igartua for inciting this research.

REFERENCES

(1) Hibbs, M. R.; Hickner, M. A.; Alam, T. M.; McIntyre, S. K.; Fujimoto, C. H.; Cornelius, C. J. Transport Properties of Hydroxide and Proton Conducting Membranes. *Chem. Mater.* **2008**, *20*, 2566−2573.

(2) Hickner, M. A. Ion-Containing Polymers: New Energy & Clean Water. *Mater. Today* **2010**, *13*, 34−41.

(3) Mecerreyes, D. Polymeric Ionic Liquids: Broadening the Properties and Applications of Polyelectrolytes. *Prog. Polym. Sci.* **2011**, *36*, 1629−1648.

(4) Toma, Š.; Mečiarová, M.; Šebesta, R. Are Ionic Liquids Suitable Media for Organocatalytic Reactions? *Eur. J. Org. Chem.* **2009**, *2009*, 321−327.

(5) Yue, C.; Fang, D.; Liu, L.; Yi, T.-F. Synthesis and Application of Task-Specific Ionic Liquids Used as Catalysts and/or Solvents in Organic Unit Reactions. *J. Mol. Liq.* **2011**, *163*, 99−121.

(6) Dupont, J.; Scholten, J. D. On the Structural and Surface Properties of Transition-Metal Nanoparticles in Ionic Liquids. *Chem. Soc. Rev.* **2010**, *39*, 1780−1804.
(7) Jiménez, A.; Bermúdez, M.-D. Ionic Liquids as Lubricants of Titanium−Steel Contact. *Tribol. Lett.* **2009**, *33*, 111−126.
(8) Mordukhovich, G.; Qu, J.; Howe, J. Y.; Bair, S.; Yu, B.; Luo, H.; Smolenski, D. J.; Blau, P. J.; Bunting, B. G.; Dai, S. A Low-Viscosity Ionic Liquid Demonstrating Superior Lubricating Performance from Mixed to Boundary Lubrication. *Wear* **2013**, *301*, 740−746.
(9) Castejón, H. J.; Wynn, T. J.; Marcin, Z. M. Wetting and Tribological Properties of Ionic Liquids. *J. Phys. Chem. B* **2014**, *118*, 3661−3668.
(10) Asencio, R. Á.; Cranston, E. D.; Atkin, R.; Rutland, M. W. Ionic Liquid Nanotribology: Stiction Suppression and Surface Induced Shear Thinning. *Langmuir* **2012**, *28*, 9967−9976.
(11) Somers, A.; Howlett, P.; MacFarlane, D.; Forsyth, M. A Review of Ionic Liquid Lubricants. *Lubricants* **2013**, *1*, 3−21.
(12) Otero, I.; López, E. R.; Reichelt, M.; Fernández, J. Friction and Anti-Wear Properties of Two Tris(Pentafluoroethyl)-trifluorophosphate Ionic Liquids as Neat Lubricants. *Tribiol. Int.* **2014**, *70*, 104−111.
(13) Minami, I. Ionic Liquids in Tribology. *Molecules* **2009**, *14*, 2286−2305.
(14) Bermúdez, M.-D.; Jiménez, A.-E.; Sanes, J.; Carrión, F.-J. Ionic Liquids as Advanced Lubricant Fluids. *Molecules* **2009**, *14*, 2888−2908.
(15) Palacio, M.; Bhushan, B. A Review of Ionic Liquids for Green Molecular Lubrication in Nanotechnology. *Tribol. Lett.* **2010**, *40*, 247−268.
(16) Pagano, F.; et al. Dicationic Ionic Liquids as Lubricants. *Proc. Inst. Mech. Eng., Part J: J. Eng. Tribol.* **2012**, *226*, 952−964.
(17) Lu, R.; Mori, S.; Kobayashi, K.; Nanao, H. Study of Tribochemical Decomposition of Ionic Liquids on a Nascent Steel Surface. *Appl. Surf. Sci.* **2009**, *255*, 8965−8971.
(18) Jiménez, A. E.; Bermúdez, M. D. Ionic Liquids as Lubricants of Titanium−Steel Contact. Part 3. Ti6al4v Lubricated with Imidazolium Ionic Liquids with Different Alkyl Chain Lengths. *Tribol. Lett.* **2010**, *40*, 237−246.
(19) Millett, W. H. Polyalkylene Glycol Synthetic Lubricants. *Ind. Eng. Chem.* **1950**, *42*, 2436−2441.
(20) Gathergood, N.; Garcia, M. T.; Scammells, P. J. Biodegradable Ionic Liquids: Part I. Concept, Preliminary Targets and Evaluation. *Green Chem.* **2004**, *6*, 166−175.
(21) Gathergood, N.; Scammells, P. J. Design and Preparation of Room-Temperature Ionic Liquids Containing Biodegradable Side Chains. *Aust. J. Chem.* **2002**, *55*, 557−560.
(22) Nevshupa, R. A.; Roman, E.; de Segovia, J. L. Contamination of Vacuum Environment Due to Gas Emission Stimulated by Friction. *Tribiol. Int.* **2013**, *59*, 23−29.
(23) Nevshupa, R. A.; de Segovia, J. L.; Deulin, E. A. Outgassing of Stainless Steel During Sliding Friction in Ultra-High Vacuum. *Vacuum* **1999**, *53*, 295−298.
(24) Nevshupa, R. A.; de Segovia, J. L. Outgassing from Stainless Steel under Impact in UHV. *Vacuum* **2002**, *64*, 425−430.
(25) Nevshupa, R.; Roman, E.; Konovalov, P.; de Segovia, J. L. New Method To Determine Gas Content in Materials. *J. Phys.: Conf. Ser.* **2008**, *100*, 072030.
(26) Rusanov, A.; Fontaine, J.; Martin, J.-M.; Le Mogne, T.; Nevshupa, R. A. Gas Desorption during Friction of Amorphous Carbon Films. *J. Phys.: Conf. Ser.* **2008**, *100*, 082050.
(27) Nevchoupa, R. A.; De Segovia, J. L.; Deulin, E. A. An UHV System To Study Gassing and Outgassing of Metals under Friction. *Vacuum* **1999**, *52*, 73−81.
(28) Řepa, P. Mechanically Induced Desorption. *Vacuum* **1992**, *43*, 367−371.
(29) Amelin, A. V.; Muinov, T. M.; Pozdnyakov, O. F.; Regel, V. R. Comparison of the Mass Spectra of the Volatile Products Liberated from Polymers in the Course of Mechanical Destruction and Thermal Degradation. *Mech. Compos. Mater.* **1967**, *3*, 54−60.
(30) Wu, C.; Peng, J.; Li, J.; Bai, Y.; Hu, Y.; Lai, G. Synthesis of Poly(ethylene glycol) (PEG) Functionalized Ionic Liquids and the Application to Hydrosilylation. *Catal. Commun.* **2008**, *10*, 248−250.
(31) Zare, P.; Mahrova, M.; Tojo, E.; Stojanovic, A.; Binder, W. H. Ethylene Glycol-Based Ionic Liquids via Azide/Alkyne Click Chemistry. *J. Polym. Sci., Part A: Polym. Chem.* **2013**, *51*, 190−202.
(32) Frech, R.; Huang, W. Conformational Changes in Diethylene Glycol Dimethyl Ether and Poly(ethylene oxide) Induced by Lithium Ion Complexation. *Macromolecules* **1995**, *28*, 1246−1251.
(33) Katsyuba, S. A.; Zvereva, E. E.; Vidiš, A.; Dyson, P. J. Application of Density Functional Theory and Vibrational Spectroscopy toward the Rational Design of Ionic Liquids. *J. Phys. Chem. A* **2006**, *111*, 352−370.
(34) Nevshupa, R. A.; de Segovia, J. L.; Roman, E. Surface-Induced Reactions of Absorbed Hydrogen under Mutual Mechanical Forces. *Vacuum* **2005**, *80*, 241−246.
(35) Peressadko, A. G.; Nevshupa, R. A.; Deulin, E. A. Mechanically Stimulated Outgassing from Ball Bearings in Vacuum. *Vacuum* **2002**, *64*, 451−456.
(36) Nevshupa, R. A.; Roman, E.; De Segovia, J. L. Origin of Hydrogen Desorption during Friction of Stainless Steel by Alumina in Ultrahigh Vacuum. *J. Vac. Sci. Technol., A* **2008**, *26*, 1218−1223.
(37) Kroon, M. C.; Buijs, W.; Peters, C. J.; Witkamp, G.-J. Quantum Chemical Aided Prediction of the Thermal Decomposition Mechanisms and Temperatures of Ionic Liquids. *Thermochim. Acta* **2007**, *465*, 40−47.
(38) Tokuda, H.; Hayamizu, K.; Ishii, K.; Susan, M. A. B. H.; Watanabe, M. Physicochemical Properties and Structures of Room Temperature Ionic Liquids. 2. Variation of Alkyl Chain Length in Imidazolium Cation. *J. Phys. Chem. B* **2005**, *109*, 6103−6110.
(39) Kiefer, J.; Fries, J.; Leipertz, A. Experimental Vibrational Study of Imidazolium-Based Ionic Liquids: Raman and Infrared Spectra of 1-Ethyl-3-methylimidazolium Bis(Trifluoromethylsulfonyl)Imide and 1-Ethyl-3-methylimidazolium Ethylsulfate. *Appl. Spectrosc.* **2007**, *61*, 1306−1311.
(40) Rey, I.; Johansson, P.; Lindgren, J.; Lassègues, J. C.; Grondin, J.; Servant, L. Spectroscopic and Theoretical Study of $(CF_3SO_2)_2N^-$ ($TFSI^-$) and $(CF_3SO_2)_2NH$ (HTFSI). *J. Phys. Chem. A* **1998**, *102*, 3249−3258.
(41) Talaty, E. R.; Raja, S.; Storhaug, V. J.; Dölle, A.; Carper, W. R. Raman and Infrared Spectra and ab Initio Calculations of C_{2-4}MIM Imidazolium Hexafluorophosphate Ionic Liquids. *J. Phys. Chem. B* **2004**, *108*, 13177−13184.
(42) Katsyuba, S. A.; Dyson, P. J.; Vandyukova, E. E.; Chernova, A. V.; Vidiš, A. Molecular Structure, Vibrational Spectra, and Hydrogen Bonding of the Ionic Liquid 1-Ethyl-3-methyl-1*H*-imidazolium Tetrafluoroborate. *Helv. Chim. Acta* **2004**, *87*, 2556−2565.
(43) Heimer, N. E.; Del Sesto, R. E.; Meng, Z.; Wilkes, J. S.; Carper, W. R. Vibrational Spectra of Imidazolium Tetrafluoroborate Ionic Liquids. *J. Mol. Liq.* **2006**, *124*, 84−95.
(44) Kitahara, Y.; Takahashi, S.; Fujii, T. Thermal Analysis of Polyethylene Glycol: Evolved Gas Analysis with Ion Attachment Mass Spectrometry. *Chemosphere* **2012**, *88*, 663−669.
(45) Yoshihara, T.; Tadokoro, H.; Murahashi, S. Normal Vibrations of the Polymer Molecules of Helical Conformation. IV. Polyethylene Oxide and Polyethylene-d_4 Oxide. *J. Chem. Phys.* **1964**, *41*, 2902−2911.
(46) Dong, H.; Hyun, J.-K.; Rhodes, C. P.; Frech, R.; Wheeler, R. A. Molecular Dynamics Simulations and Vibrational Spectroscopic Studies of Local Structure in Tetraglyme:Sodium Triflate (CH_3O-$(CH_2CH_2O)_4CH_3$:$NaCF_3SO_3$) Solutions. *J. Phys. Chem. B* **2002**, *106*, 4878−4885.
(47) Shimanouchi, T.; Matsuura, H.; Ogawa, Y.; Harada, I. Tables of Molecular Vibrational Frequencies. *J. Phys. Chem. Ref. Data* **1978**, *7*, 1323−1444.
(48) Pielichowski, K.; Flejtuch, K. Non-Oxidative Thermal Degradation of Poly(ethylene oxide): Kinetic and Thermoanalytical Study. *J. Anal. Appl. Pyrolysis* **2005**, *73*, 131−138.

(49) Han, S.; Kim, C.; Kwon, D. Thermal/Oxidative Degradation and Stabilization of Polyethylene Glycol. *Polymer* **1997**, *38*, 317−323.
(50) Gao, J.; Chen, L.; He, Y. Y.; Yan, Z. C.; Zheng, X. J. Degradation of Imidazolium-Based Ionic Liquids in Aqueous Solution Using Plasma Electrolysis. *J. Hazard. Mater.* **2014**, *265*, 261−270.
(51) Cheng U, C.; Stair, P. C. In Situ Study of Multialkylated Cyclopentane and Perfluoropolyalkyl Ether Chemistry in Concentrated Contacts Using Ultraviolet Raman Spectroscopy. *Tribol. Lett.* **1998**, *4*, 163−170.
(52) Kennedy, F. E., Frictional Heating and Contact Temperatures. In *Modern Tribology Handbook*; Bhushan, B., Ed.; Taylor & Francis: Abingdon, U.K., 2010; pp 235−272.
(53) Nevshupa, R. The Role of Athermal Mechanisms in the Activation of Tribodesorption and Triboluminisence in Miniature and Lightly Loaded Friction Units. *J. Frict. Wear* **2009**, *30*, 118−126.
(54) Butyagin, P. Y. Problems in Mechanochemistry and Prospects for Its Development. *Russ. Chem. Rev.* **1994**, *63*, 965.
(55) Palacio, M.; Bhushan, B. Molecularly Thick Dicationic Ionic Liquid Films for Nanolubrication. *J. Vac. Sci. Technol., A* **2009**, *27*, 986−995.
(56) Nainaparampil, J. J.; Phillips, B. S.; Eapen, K. C.; Zabinski, J. S. Micro−Nano Behaviour of DMBI-PF_6 Ionic Liquid Nanocrystals: Large and Small-Scale Interfaces. *Nanotechnology* **2005**, *16*, 2474.
(57) Valkenberg, M. H.; deCastro, C.; Holderich, W. F. Immobilisation of Ionic Liquids on Solid Supports. *Green Chem.* **2002**, *4*, 88−93.
(58) Zhurkov, S. N. Problem of Strength of Solids. *Vestn. Akademii Nauk SSSR* **1957**, *11*, 78−82.
(59) Fernández, L. E.; Varetti, E. L. An Experimental and Theoretical Study of the Vibrational Properties of CF_3SO_2Cl. *J. Argent. Chem. Soc.* **2009**, *97*, 199−209.
(60) Gonbeau, D.; Guimon, M. F.; Duplantier, S.; Ollivier, J.; Pfister-Guillouzo, G. Sulfochloration of Trifluoromethane. Theoretical Study of the Trifluoromethane Sulfonyl Radical. *Chem. Phys.* **1989**, *135*, 85−89.
(61) Shah, J. K.; Maginn, E. J. Molecular Dynamics Investigation of Biomimetic Ionic Liquids. *Fluid Phase Equilib.* **2010**, *294*, 197−205.